

Implementation of NMR quantum computation with *para*-hydrogen derived high purity quantum states

M. S. Anwar* and J. A. Jones†

*Centre for Quantum Computation, Clarendon Laboratory,
University of Oxford, Parks Road, OX1 3PU, United Kingdom*

D. Blazina‡ and S. B. Duckett§

Department of Chemistry, University of York, Heslington, York, YO10 5DD, United Kingdom

H. A. Carteret¶

*LITQ, Département d'Informatique et Recherche Opérationnelle,
Pavillon André-Aisenstadt, Université de Montréal, Montréal, Québec H3C 3J7, Canada*

(Dated: December 6, 2018)

We demonstrate the first implementation of a quantum algorithm on a liquid state nuclear magnetic resonance (NMR) quantum computer using almost pure states. This was achieved using a two qubit device where the initial state is an almost pure singlet nuclear spin state of a pair of ^1H nuclei arising from a chemical reaction involving *para*-hydrogen. We have implemented Deutsch's algorithm for distinguishing between constant and balanced functions with a single query.

PACS numbers: 03.67.Lx, 82.56.-b, 03.67.Mn

I. INTRODUCTION

The practical implementation of quantum algorithms has so far been dominated by liquid state nuclear magnetic resonance (NMR) [1, 2, 3] techniques [4, 5, 6, 7, 8, 9, 10]. The many algorithms successfully implemented on liquid state NMR systems include, most notably, Deutsch's algorithm [6, 7], Grover's quantum search [8, 9], and Shor's factoring algorithm [10]. This unrivalled success can be attributed to the high degree of coherent control over small spin systems and also to the long decoherence times in comparison with the timescales of the computation. However, one of the problems haunting the prospects of liquid state NMR as a practically scalable and "truly quantum" implementation, was that the states encountered in *almost all* of the previous implementations were highly mixed [11, 12].

The highly mixed states used in NMR raised two major concerns. First, there was the issue of initializing the spins into a well-defined state [13, 14]. It was shown that one could circumvent this problem [4, 5] by preparing pseudopure states [15, 16, 17], which behave *effectively* (up to a certain scaling factor) as pure states. This approach worked well for small spin systems, but cannot be extended to larger systems, because of the exponential loss in signal with increase in the number of spins [12, 14]. Secondly, the highly mixed states encountered in conventional liquid state NMR are separable [11]. As entan-

glement could not exist in these systems, some authors suggested that NMR quantum computing could perhaps be explained using classical models [18]. With separable states, even the quantum nature of NMR quantum computing was under question!

Motivated by these problems, we have previously demonstrated [19] the preparation of an almost pure two-spin state, which lies above the entanglement threshold [20, 21], for the two hydride ^1H nuclei in the organometallic compound $\text{Ru}(\text{H})_2(\text{CO})_2(\text{dppe})$, where dppe indicates 1,2-bis(diphenylphosphino)ethane. This was achieved using laser induced addition of pure *para*-hydrogen to $\text{Ru}(\text{CO})_2(\text{dppe})$ as discussed below. We now describe an implementation of the Deutsch algorithm on this spin system, demonstrating that coherent manipulations of spins in our pure spin system can also be carried out.

Our experiments solve the two-fold problem of initialization and separability. We bypass the need for preparing pseudopure states, as our computation starts off directly with an almost pure Werner state [22]. Furthermore, the initial purity of the system lies above the entanglement threshold. We do not claim that our implementation *actually* involves entangled states—only that entanglement can be distilled from these states. The use of entanglement proper in the Deutsch's algorithm has been discussed in more detail elsewhere [23]. In short, the current work constitutes the first demonstration of a quantum algorithm in liquid state NMR using an almost pure initial state.

The remainder of the paper is organized as follows. In section II we describe the use of *para*-hydrogen to generate spin systems in almost pure initial states, while in section III we give a brief summary of Deutsch's problem and the quantum algorithm devised to solve it. Liquid state NMR can be used to implement the algorithm as with our two spin pure state; this is discussed in section

*Electronic address: muhammad.anwar@physics.ox.ac.uk

†Electronic address: jonathan.jones@qubit.org

‡Electronic address: db30@york.ac.uk

§Electronic address: sbd3@york.ac.uk

¶Electronic address: cartereh@iro.umontreal.ca

IV and the experimental procedures and results are described in section V. Finally, we present a concluding summary in section VI and also outline some possible directions for future work.

II. PARA-HYDROGEN

The high spin-state purity in our experiment is a result of an effect called *para*-hydrogen induced polarization (PHIP) [24, 25, 26, 27]. The existence of the *para* spin isomer of dihydrogen molecules, H_2 , is a consequence of the Pauli principle and the symmetrization postulate [28]. These require the overall wavefunction of the H_2 molecule to be antisymmetric with respect to interchange of the fermionic 1H nuclei. The translational and vibrational wavefunctions of H_2 are always symmetric, as is the ground state electronic wavefunction, and so overall antisymmetry is achieved by choosing the rotational and nuclear spin wavefunctions such that their product is antisymmetric. It follows that H_2 molecules in even rotational states ($J = 0, 2, \dots$) possess an antisymmetric nuclear spin wave function and correspond to nuclear spin singlets, termed *para*; similarly, H_2 molecules in odd rotational states ($J = 1, 3, \dots$) possess a symmetric nuclear spin wave function and correspond to nuclear spin triplets, termed *ortho*.

Interconversion of the two spin-state isomers of hydrogen is normally forbidden by angular momentum selection rules, but in the presence of a paramagnetic catalyst the symmetry of the H_2 system is broken, allowing these rules to be overcome. Thus if hydrogen is cooled in the presence of an appropriate catalyst, it will become enriched in the (low energy) *para* form. Upon moving away from the catalyst interconversion is again suppressed, and so the *ortho/para* ratio in effect *remembers* the temperature of the last conversion surface encountered. A temperature of 20 K is sufficiently low to cool 99.8% of H_2 molecules into the $J = 0$ state [26] and hence produce essentially pure *para*-hydrogen.

The sole antisymmetric state of two 1H nuclei is the singlet state, and so pure *para*-hydrogen will *also* have a pure nuclear spin singlet state. This ability to prepare a pure initial state is obviously attractive for NMR quantum computing experiments, but the *para*-hydrogen molecule cannot be used directly for NMR quantum computing, as it is NMR silent due to its high symmetry. This can be overcome by means of a chemical reaction, producing a new molecule, in which the two hydrogen atoms can be made distinct (I and S) and *can* be separately addressed. In conventional *para*-hydrogen experiments the chemical reaction is slow in comparison with the frequency difference between the I and S spins of the reaction product. This causes the off-diagonal terms in the density matrix to dephase, producing a separable state. This dephasing can be overcome (neglecting relaxation) [29] by applying an isotropic mixing sequence [30], but a much simpler approach is to ensure that the

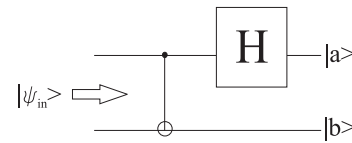


FIG. 1: Disentangling network, rotating Bell states into eigenstates.

reaction is rapid in comparison with the dephasing and relaxation timescales. We achieve this through addition of *para*-hydrogen to a highly reactive species, generated by laser flash photolysis of a stable precursor.

The state that we actually prepare in our *para*-hydrogen experiments is observed to be a Werner singlet state [22] of the form

$$\rho_{init} = (1 - \varepsilon)\frac{\mathbb{1}}{4} + \varepsilon|\psi^-\rangle\langle\psi^-|, \quad (1)$$

where $|\psi^-\rangle$ is the singlet vector, which can be written in the computational basis as

$$|\psi^-\rangle = \frac{1}{\sqrt{2}}(|01\rangle - |10\rangle), \quad (2)$$

and the polarization ε determines the purity, with $\varepsilon = 1$ corresponding to the pure state; for our system [19] $\varepsilon \approx 0.92$, and so the state is almost pure. The singlet state is one of the four Bell states [31], $|\phi^\pm\rangle = (|00\rangle \pm |11\rangle)/\sqrt{2}$ and $|\psi^\pm\rangle = (|01\rangle \pm |10\rangle)/\sqrt{2}$, all of which can be interconverted using local unitary transformations [31, 32]. The Bell states can also be converted to basis vectors in the computational basis (the usual starting point for quantum computations) using a network of the form given in Figure 1, which is a disentangling network. The output qubit $|a\rangle$ is determined by the label (ϕ or ψ) of the input state $|\psi_{in}\rangle$ and $|b\rangle$ is determined by the sign (+ or -); eigenstates can be converted back to the Bell states, using the reverse of the circuit in Fig. 1, and the mapping can be compactly expressed as

$$|a\rangle|b\rangle \longleftrightarrow \frac{1}{\sqrt{2}}(|0\rangle|b\rangle + (-1)^a|a\rangle|\neg b\rangle), \quad (3)$$

where $|\neg b\rangle$ is the classical NOT of $|b\rangle$. With circuits built around the disentangling circuit, we can achieve conventional two qubit initial states, starting off from $|\psi_{in}\rangle = |\psi^-\rangle$.

III. THE DEUTSCH PROBLEM

Deutsch's problem [33] was the first problem to be solved by a quantum algorithm. Although its usefulness as a real-life problem is limited, it is nevertheless a convenient testing ground for quantum computation. A refined version of Deutsch's problem [34] is described in the following way.

x	$f_{00}(x)$	$f_{01}(x)$	$f_{10}(x)$	$f_{11}(x)$
0	0	0	1	1
1	0	1	0	1

TABLE I: Truth table for the four single-bit functions.

Suppose we are given a binary string $\mathbf{s} = \{0, 1\}^n$ of length n and a binary function f acting on \mathbf{s} mapping it onto a single bit, 0 or 1, *i.e.*, $f : \{0, 1\}^n \rightarrow \{0, 1\}$. Furthermore, we are *promised* that f is either constant or balanced. (A constant f outputs the *same* value, either 1 or 0, for all 2^n possible input strings \mathbf{s} , whereas a balanced f outputs 0 for exactly half of the strings and 1 for the other half.) The problem is then to find whether f is constant or balanced using the minimum number of queries. In the classical setting, answering this question, in the worst case, would require $(2^n/2) + 1$ queries. However, with a quantum algorithm it is possible to solve this problem in a single query, giving an exponential improvement over the worst-case classical version.

The simplest form of Deutsch's problem concerns the case of $n = 1$, with functions mapping a single bit onto a single bit, $f : \{0, 1\} \rightarrow \{0, 1\}$. There are four such functions, their operation being described by the truth table given in Table I. Out of these four functions, two are constant (f_{00} and f_{11}) and two are balanced (f_{01} and f_{10}). Classically the problem is solved by evaluating *first* $f(0)$ and *then* $f(1)$ and comparing the results. Equivalently, f is constant if $f(0) \oplus f(1) = 0$ and balanced if $f(0) \oplus f(1) = 1$, where \oplus indicates addition modulo 2. Deutsch's algorithm enables us to find this global property of f in a *single* query.

The conventional approach to solve the single-bit problem is to use two input and two output qubits and then implement f using carefully selected reversible gates. These gates are represented by the propagators U_f , whose action on the input qubits can be expressed as

$$|x\rangle|y\rangle \xrightarrow{U_f} |x\rangle|f(x) \oplus y\rangle, \quad (4)$$

leaving the first qubit unchanged. If $|y\rangle$ is initialized as $|0\rangle$, the second qubit holds the value of $f(x)$ after the computation,

$$|x\rangle|0\rangle \xrightarrow{U_f} |x\rangle|f(x)\rangle. \quad (5)$$

There are four propagators, U_{00} , U_{01} , U_{10} and U_{11} , corresponding to the four different functions. A suitable choice of propagators is

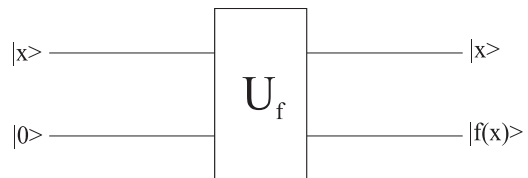
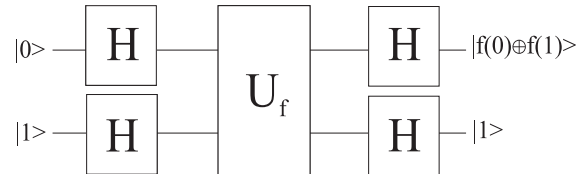
$$U_{00} = \mathbb{1} \otimes \mathbb{1} \quad (6)$$

$$U_{01} = |0\rangle\langle 0| \otimes \mathbb{1} + |1\rangle\langle 1| \otimes \sigma_x \quad (7)$$

$$U_{10} = |0\rangle\langle 0| \otimes \sigma_x + |1\rangle\langle 1| \otimes \mathbb{1} \quad (8)$$

$$U_{11} = \mathbb{1} \otimes \sigma_x \quad (9)$$

where $\mathbb{1}$ is the unit matrix of order 2 and σ_x is a Pauli spin matrix [31]. It is straightforward to check that with

FIG. 2: Quantum circuit for the classical evaluation of $f(x)$.FIG. 3: Quantum circuit for solving Deutsch's problem. H represents a Hadamard gate.

appropriate initial states these propagators indeed reproduce the transformation given in Equation 5. In the usual language of quantum networks U_{00} is a do-nothing gate; U_{01} is a 1-controlled-NOT gate; U_{10} is a 0-controlled-NOT gate and U_{11} is a NOT gate on the second qubit. (Reference [35] contains a concise description of quantum logic gates in NMR).

We can build a quantum circuit from these propagators, which is depicted in block form in Figure 2. With this network, the second qubit evaluates $f(x)$, although the evaluation is classical and we still need *two* separate evaluations to determine the nature of f , once with $x = 0$ and once with $x = 1$. This circuit is, however, useful for illustrative purposes. For example, using this circuit one could verify the truth table in Table I. To solve Deutsch's problem in a single step, however, we exploit superposition states, preparing them from the eigenstates using Hadamard gates [31]. The corresponding network is given in Figure 3, and the algorithm proceeds as follows: the computation starts off in the state $|0\rangle \otimes |1\rangle$, the Hadamard gates prepare the superposition state, followed by the unitary transformation U_f , and the final Hadamard gates then convert the superpositions back to eigenstates, with the first qubit ending in $f(0) \oplus f(1)$ —the solution to the problem!

IV. IMPLEMENTING THE ALGORITHM

We have implemented the Deutsch algorithm on an almost pure ($\varepsilon \approx 0.92$) two qubit state using an NMR quantum computer. We also evaluated $f(x)$ classically using the procedure already outlined. In an NMR quantum computer, the qubits are spin-1/2 atomic nuclei (in this case ^1H nuclei) placed in a strong magnetic field, and the gates are implemented through a sequence of radio-frequency (RF) pulses, interspersed with properly

timed delays, during which the spin system evolves under its own Hamiltonian. Details may be found in reviews of quantum computing with liquid state NMR, such as [35, 36, 37, 38]. Here we use product operator notation [1, 39, 40] for the states and propagators. Pulse sequences are written from left to right and we label the two spins as I and S , in keeping with NMR parlance. The notation θ_α is used to represent a rotation by θ° about the α axis.

To implement the classical and quantum versions of the problem (Figures 2 and 3), the individual gates have to be built from RF pulses and frame rotations. For example, the Hadamard gate on a single qubit is a 180° rotation about a tilted axis [35] and can be achieved using the sequence $180_z 90_{-y}$. Pulse sequences can also be simplified based on the properties of product operators: for example, if the Hadamard acts on an eigenstate, the initial z -pulse can be dropped out as these states commute with z -pulses. We are therefore simply left with 90_{-y} pseudo-Hadamard operations which can be used as a simpler replacement for proper Hadamard gates. Likewise, if a computation ends in a diagonal state, we can shift the 180_z pulses to the end (right) of the sequence, changing, of course, the phase of the 90° pulses, and *collapse* the z -pulse with the final state. We are then left with a simple 90_y pulse in place of a strict Hadamard. In the same spirit, the z -rotations can be moved within a sequence, either to the left or to the right, and can be viewed as rotations of the reference frame, often referred to as the abstract reference frame [17]. We have used the abstract frames approach together with composite z -rotations [41] to simplify our sequences.

The unitary transformations corresponding to the four possible U_f 's are given in Equations 6–9. U_{00} is an identity gate, and translates to “do nothing”, while U_{11} is a selective NOT gate on the second qubit, $180S_x$. The remaining two transformations, U_{01} and U_{10} can be expressed in product operator notation as, for example,

$$90S_{-y} 90I_z 90S_z (-90)2I_z S_z 90S_y \quad (10)$$

and

$$90S_{-y} 90I_{-z} 90S_z (90)2I_z S_z 90S_y \quad (11)$$

respectively. These transformations involve frame rotations, evolution under scalar coupling terms ($2I_z S_z$) and soft pulses [3], selectively exciting the S spin. Selective pulses were implemented using the Jump and Return pulses described previously [42], so that our final simplified sequences comprise only hard pulses and delays. The sequences for the non-trivial transformations, U_{01} , U_{10} and U_{11} are

$$P_{01} = 90_{-x}[\tau_1]90_{45}[2\tau_1 + \tau_2]180_x[\tau_2]90_{135}[\tau_1]90_{-x} \quad (12)$$

$$P_{10} = 90_x[\tau_1]90_{45}[2\tau_1 + \tau_2]180_x[\tau_2]90_{135}[\tau_1]90_x \quad (13)$$

$$P_{11} = 90_y[2\tau_1]90_{-y}90_x \quad (14)$$

where $\tau_1 = 1/4\delta$ and $\tau_2 = 1/4J$, δ being the frequency separation between the spin resonances and J the spin-spin coupling constant, both measured in Hz.

a	b	Pulse sequence
0	0	$\mathbf{A} \equiv [\tau_1]90_y[\tau_2]180_x[\tau_2]180_y[\tau_1]90_x$
0	1	$\mathbf{B} \equiv [\tau_1]90_y[\tau_2]180_x[\tau_2]90_y$
1	0	$\mathbf{C} \equiv [\tau_1]90_y[\tau_2]180_x[\tau_2]90_{-y}$

TABLE II: Pulse sequences for mapping the singlet state $|\psi^-\rangle$ onto the input states $|ab\rangle$.

We have so far overlooked another important issue, the preparation of initial states. The *para*-hydrogen derived state is an almost pure singlet, but the algorithms expect the quantum computer to begin in some eigenstate $|ab\rangle$, with the values of a and b depending on the algorithm. With circuits built around the disentangling circuit, Fig. 1, we can achieve the desired input states, starting off from $|\psi_{in}\rangle = |\psi^-\rangle$. The simplified pulse sequences to accomplish this transformation are shown in Table II.

Implementation of the classical and Deutsch algorithms involves preparing the almost pure state $|\psi^-\rangle$, converting it into the desired initial state using a recipe from Table II, and applying the appropriate pulse sequence for the algorithm. Finally, we need to read out the result at the end of the computation. At this stage the output states are diagonal, and so cannot be directly observed, but a simple hard 90_y acquire pulse rotates these states to the measurement basis: the $|0\rangle$ state gives an NMR signal I_x (positive absorption) and $|1\rangle$ gives a signal $-I_x$ (negative absorption). The output states can, therefore, be unambiguously assigned as $|0\rangle$ or $|1\rangle$ by examining the two multiplets.

V. THE EXPERIMENT

The two qubit system for our NMR quantum computer comprises the two hydride ^1H nuclei in the organometallic compound $\text{Ru}(\text{H})_2(\text{CO})_2(\text{dppe})$, where dppe indicates 1,2-bis(diphenylphosphino)ethane and the hydride hydrogen atoms are derived from *para*-hydrogen. We prepared essentially pure *para*-hydrogen at a temperature of 18 K in the presence of a charcoal-based catalyst. The gas was introduced into a 5 mm NMR tube containing the precursor compound $\text{Ru}(\text{CO})_3(\text{dppe})$, dissolved in d_6 -benzene. The preparation of the precursor and finer experimental details are identical to previous work [19, 43, 44]. The NMR tube was then transferred into a 400 MHz spectrometer fitted with a $^1\text{H}/^{31}\text{P}$ probe modified for *in situ* photolysis [44]. The spectrometer triggered an MPB Technologies MSX-250 pulsed XeCl excimer laser which fired a 12 ns UV pulse of wavelength 308 nm, irradiating the active region of the NMR sample and producing the unstable species $\text{Ru}(\text{CO})_2(\text{dppe})$. This unstable intermediate reacts with dissolved *para*-hydrogen on the sub-microsecond timescale [45] leading to the product of interest, $\text{Ru}(\text{H})_2(\text{CO})_2(\text{dppe})$. The two hydrogen nuclei which inherit the pure singlet spin state

Experiment	Pulse sequence
Classical $f(0)$	A — G — U_f — 90_y
Classical $f(1)$	C — G — U_f — 90_y
Quantum $f(0) \oplus f(1)$	B — G — 90_y — U_f

TABLE III: Pulse sequences for the Deutsch algorithm. Gradient fields are represented by **G**.

from the *para*-hydrogen comprise the two qubits of our quantum computer.

The hydride resonances appear at -7.55 ppm (spin I) and -6.32 ppm (spin S), with a frequency separation of $\delta = 492$ Hz. The ^1H transmitter frequency was placed exactly between the two resonance frequencies, and couplings to ^{31}P nuclei were removed by GARP decoupling [46] applied continuously throughout the experiments. The T_1 and T_2 constants for the hydride peaks were measured to be 1.7 and 0.58 s respectively while the hydride J coupling ($^2J_{\text{HH}}$) was 4.6 Hz. The laser flash acts as an initialisation switch, generating the pure state $|\psi_{in}\rangle = |\psi^-\rangle$ on demand, which is subsequently used for the implementation. The pulse sequences for the classical and quantum evaluations are described below and summarized in Table III.

Using our system, we were able to analyze $f(0)$ and $f(1)$, corresponding to the classical evaluation of these functions (see Figure 2). For example, for the determination of $f(0)$ the initial state $|00\rangle$ can be prepared from the singlet state $|\psi^-\rangle$ using the sequence **A** (see Table II). At this stage, we clean our state by applying a strong field gradient [3, 40]; this will not affect the component of the state in the desired eigenstate, but the majority of unwanted terms will be dephased [9]. We then apply the transformation U_f and finally measure with a 90_y acquire pulse. The resulting spectra for the four possible choices of U_f are shown in Figure 4. From Table I, we observe that $f(0) = 0$ for f_{00} and f_{01} and $f(0) = 1$ for f_{10} and f_{11} ; the result is encoded in the state of spin S (on the left), whereas spin I (on the right) remains in the state $|0\rangle$. Thus we should obtain two kinds of spectra, corresponding to $I_x \pm S_x$, with the I resonance in positive absorption and the S resonance in positive or negative absorption, depending on the value of $f(x)$. The two kinds of spectra are clearly seen (Figure 4).

In the same way we evaluated $f(1)$ by converting the singlet state into $|10\rangle$ using the sequence **C** and a strong gradient field, applying the operation U_f and the acquire 90_y pulse, and observing the result; spectra are shown in Figure 5. We again observe two kinds of spectra, $-I_x \pm S_x$: spin I is always in negative absorption and S changes phase, encoding the value of $f(1)$. Our results are in complete accord with Table I.

Finally, we implemented the quantum Deutsch algorithm using the sequence **B**, followed by the gradient, a pseudo-Hadamard and the transform U_f . An additional simplification occurs in the quantum version: the final pseudo-Hadamard can be cancelled with a 90_y acquire

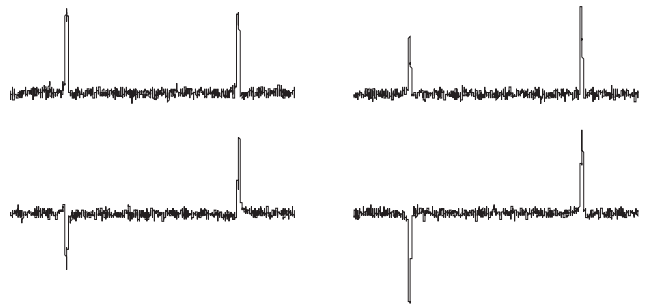


FIG. 4: Results of the algorithm for the classical determination of $f(0)$. (a) The result of applying U_{00} . The spectrum corresponds to $I_x + S_x$ and both spins are in positive absorption. This spectrum can also serve as reference for the phasing. (b) The result of applying U_{01} , corresponding again to $I_x + S_x$. (c): The result of applying U_{10} . The spectrum now corresponds to $I_x - S_x$, the left spin I is still in positive absorption and the right spin S is now inverted. (d) The result of applying U_{11} , corresponding to $I_x - S_x$. Spin I always remains in positive absorption whereas S changes sign according to $f(0)$.

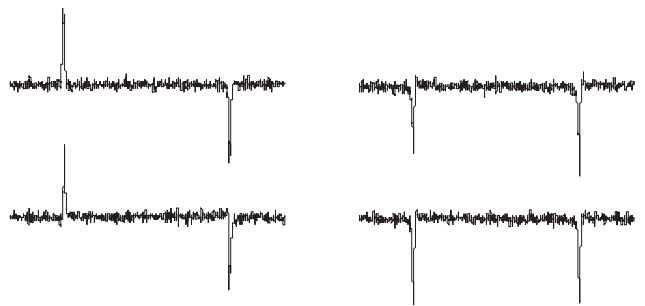


FIG. 5: Results of the algorithm for the classical determination of $f(1)$. Labelling and interpretation are the same as in Figure 4. Spin I always remains in negative absorption whereas $f(1)$ determines the sign of the signal from spin S .

pulse and the two pulses can therefore be dropped altogether. The system is, therefore, already in the measurement basis after the transformation U_f and can be observed directly. The resulting spectra are shown in Figure 6. The observed states after the quantum evaluation are $I_x - S_x$ and $-I_x - S_x$, for the constant (f_{00} , f_{11}) and balanced (f_{01} , f_{10}) functions respectively.

Although the overall results are clear, our spectra show several imperfections. Each multiplet should in principle show a perfect absorption lineshape (either positive or negative), and all the multiplets in all the spectra should ideally have the same intensity. In fact dispersive components are clearly visible, and there are considerable variations in multiplet intensities, both within spectra and between spectra. These imperfections are most pronounced in the spectra involving U_{01} and U_{10} , which were obtained with the longest and most complicated pulse sequences. The distortions can arise from many factors

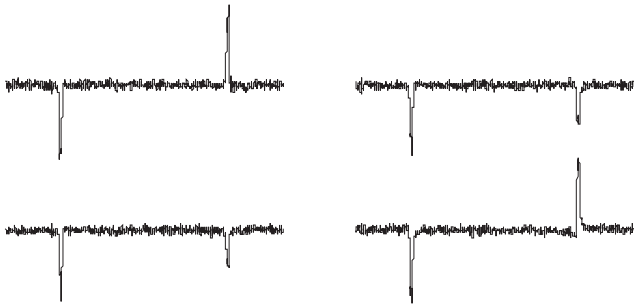


FIG. 6: Results of the algorithm for the quantum determination of $f(0) \oplus f(1)$. Labelling and interpretation are the same as in Figure 4. Spin S always remains in negative absorption while the sign of the signal from spin I encodes the final result.

such as finite coupling evolution during delays, RF inhomogeneities, miscalibrated pulses and decoherence.

To simulate the effect of decoherence under both T_1 and T_2 relaxation processes, we employed a model based on the operator sum representation [10, 31] for phase and generalized amplitude damping. The model is crude and assumes independent uncorrelated relaxation processes, but is nonetheless useful in obtaining a rough first estimate of the effects of decoherence. We observe that the damping processes should result not only in an overall decrease in the signal intensity, but for the case of the U_{01} and U_{10} propagators can also lead to intensity imbalances within a spectrum: for experiments involving these two propagators one of the spins spends more time in the transverse plane than the other, and is therefore more prone to phase damping. In the worst cases, this can cause an overall intensity imbalance of about 2 : 3, similar to the observed ratios. However for a small two qubit system such as ours, the effects of decoherence are not big enough to obscure the measurement results. Comparing the intensities of the final spectra with the intensity of spectra obtained from the initial singlet state,

we estimate the purity of the final state to be about 50 to 60 percent, indicating that we remain above the entanglement threshold throughout the implementation.

VI. CONCLUSIONS AND FUTURE WORK

We have demonstrated an implementation of the Deutsch algorithm to distinguish between constant and balanced functions using an NMR quantum computer with an almost pure initial state. We have also used the same system for classical evaluations of the function values. Unlike previous implementations built around pseudopure states, our implementation uses almost pure states which can be made on demand by laser flash photolysis. Our earlier work [19] suggested that we could get around the problem of low initial polarizations in liquid state NMR by making high purity states using the *para*-hydrogen approach. The present experiment is one step forward in showing that the high polarizations can be put to use in the form of a demonstrable quantum algorithm.

It seems that NMR quantum computing with pure states could *in principle* be scalable, although more work is needed to verify the validity (or otherwise) of this claim. We are seeking to extend this work to larger spin systems and more complex algorithms using a combination of direct *para*-hydrogen induced polarization and the transfer of spin-state purity between different spins. We are also investigating the possibility of using *para*-hydrogen techniques to reset qubits midway through a quantum computation, thus permitting repeated error correction schemes.

Acknowledgments

We thank the EPSRC for financial support. MSA thanks the Rhodes Trust for a Rhodes Scholarship. HAC thanks MITACS for financial support.

-
- [1] R. R. Ernst, G. Bodenhausen, and A. Wokuan, *Principles of Nuclear Magnetic Resonance in One and Two Dimensions* (Clarendon Press, Oxford, 1987).
 - [2] M. H. Levitt, *Spin Dynamics: Basics of Nuclear Magnetic Resonance* (John Wiley & Sons, 2001).
 - [3] R. Freeman, *Spin Choreography: Basic Steps in High Resolution NMR* Oxford University Press, Oxford (1998).
 - [4] D. G. Cory, A. F. Fahmy and T. F. Havel, in "PhysComp '96" (T. Toffoli, M. Biafore and J. Leão, Eds.), pp. 87–91, New England Complex Systems Institute (1996)
 - [5] D. G. Cory, A. F. Fahmy, and T. F. Havel, Proc. Natl. Acad. Sci. USA **94**, 1634 (1997).
 - [6] J. A. Jones, and M. Mosca, J. Chem. Phys. **109**, 1648 (1998).
 - [7] I. L. Chuang, L. M. K. Vandersypen, X. Zhou, D. W. Leung and S. Lloyd, Nature **393**, 143 (1998).
 - [8] I. L. Chuang, N. Gershenfeld, and M. Kubinec, Phys. Rev. Lett **80**, 3408 (1998).
 - [9] J. A. Jones, M. Mosca, and R. H. Hansen, Nature **393**, 344 (1998).
 - [10] L. M. K. Vandersypen, M. Steffen, G. Breyta, C. S. Yannoni, M. H. Sherwood, and I. L. Chuang, Nature **414**, 883 (2001).
 - [11] S. L. Braunstein, C. M. Caves, R. Jozsa, N. Linden, S. Popescu, and R. Schack, Phys. Rev. Lett. **83**, 1054 (1999).
 - [12] W. S. Warren, Science **277**, 229 (1997).
 - [13] D. P. DiVincenzo, Fort. der Physik **48**, 771 (2000).
 - [14] J. A. Jones, Fort. der Physik **48**, 909 (2000).
 - [15] N. A. Gershenfeld, and I. L. Chuang, Science **275**, 350 (1997).
 - [16] E. Knill, I. Chuang, and R. Laflamme, Phys. Rev. A **57**,

- 3348 (1998).
- [17] E. Knill, R. Laflamme, and C.-H. Tseng, *Nature* **404**, 368 (2000).
- [18] R. Schack, and C. M. Caves, *Phys. Rev. A* **60**, 4354, 1999.
- [19] M. S. Anwar, D. Blazina, H. A. Carteret, S. B. Duckett, T. K. Halstead, J. A. Jones, C. M. Kozak, and R. J. K. Taylor, *Phys. Rev. Lett.* (in press), quant-ph/0312014.
- [20] A. Peres, *Phys. Rev. Lett.* **77**, 1413, (1996), quant-ph/9604005.
- [21] M. Horodecki, P. Horodecki, and R. Horodecki, *Physics Letters A*. **223**, 1, (1996), quant-ph/9605038.
- [22] R. F. Werner, *Phys. Rev. A* **40**, 4277 (1989).
- [23] D. Collins, K. W. Kim, and W. C. Holton, *Phys. Rev. A*. **58**, R1633, (1998).
- [24] C. R. Bowers, and D. P. Weitekamp, *Phys. Rev. Lett.* **57**, 2645, (1986).
- [25] J. Natterer, and J. Bargon, *Prog. NMR Spectrosc.* **31**, 293, (1997).
- [26] S. B. Duckett, and C. J. Sleight, *Prog. NMR Spectrosc.* **34**, 71, (1999).
- [27] S. B. Duckett, and D. Blazina, *Eur. J. Inorg. Chem.* **16**, 2901, (2003).
- [28] A. Messiah, *Quantum Mechanics* Vol. 2, (North-Holland Publishing Company, Amsterdam, pp. 593, 2000).
- [29] P. Hübler, J. Bargon, and S. J. Glaser, *J. Chem. Phys.* **113**, 2056 (2000).
- [30] M. H. Levitt, R. Freeman, and T. Frenkiel, *J. Magn. Reson.* **47**, 328 (1982).
- [31] M. A. Nielsen and I. L. Chuang, *Quantum Computation and Quantum Information* (Cambridge University Press, 2000).
- [32] K. Mattle, H. Weinfurter, P. G. Kwiat, and A. Zeilinger, *Phys. Rev. Lett.* **76**, 4656, (1996).
- [33] D. Deutsch, and R. Jozsa, *Proc. R. Soc. London Ser. A* **439**, 553, (1992).
- [34] R. Cleve, A. Ekert, C. Macchiavello, and M. Mosca, *Proc. R. Soc. London Ser. A* **454**, 339, (1998).
- [35] J. A. Jones, R. H. Hansen, and M. Mosca, *J. Mag. Reson.* **135**, 353-36, (1998).
- [36] D. G. Cory, R. Laflamme, E. Knill, L. Viola, T. F. Havel, N. Boulant, G. Boutis, E. Fortunato, S. Lloyd, R. Martinez, C. Negreveregne, M. Pravia, Y. Sharf, G. Teklemariam, Y. S. Weinstein, and W. H. Zurek, *Fortschr. Phys.* **48**, 875, (2000).
- [37] J. A. Jones, *Prog. Nucl. Magn. Reson. Spectrosc.* **38**, 325 (2001).
- [38] L. M. K. Vandersypen, and I. L. Chuang, quant-ph/0404064, (2004).
- [39] O. W. Sørensen, G. W. Eich, M. H. Levitt, G. Bodenhausen, and R. R. Ernst, *Prog. Nucl. Magn. Reson. Spectrosc.* **16**, 163 (1983).
- [40] P. Hore, J. A. Jones, and S. Wimperis, *NMR: The Toolkit* (Oxford Chemistry Primers, Oxford, 2000).
- [41] H. Cummins, and J. A. Jones, *New J. Phys.* **2**, 6.1, (2000).
- [42] J. A. Jones, and M. Mosca, *Phys. Rev. Lett.* **83**, 1050 (1999).
- [43] D. Schott, C. J. Sleight, J. P. Lowe, S. B. Duckett, R. J. Mawby, and M. G. Partridge, *Inorg. Chem.* **41**, 2960, (2002).
- [44] C. Godard, P. Callaghan, J. L. Cullingham, S. B. Duckett, J. A. B. Lohman, and R. N. Perutz, *Chem. Comm.* **23**, 2386, (2002).
- [45] L. Cronin, M. C. Nicasio, R. N. Perutz, R. G. Peters, D. M. Roddick, and M. K. Whittlesey, *J. Am. Chem. Soc.* **117**, 10047, (1995).
- [46] A. J. Shaka, P. B. Barker, and R. Freeman, *J. Magn. Reson.* **64**, 547, (1985).